Modeling the Effects of Cannibalistic Behavior in Zebra Mussel (*Dreissena polymorpha*) Populations

Patrick T. Davis
Eastern Michigan University

Dr. May Boggess (Texas A&M University)
Dr. Jay Walton (Texas A&M University)

Summer 2010

Abstract

The threat of invasive species has increased with the expansion of global transportation. In the United States, zebra mussels became a problem by the early 1990's when they were introduced by ballast water into Lake St. Clair in 1988. In 2007, a new deterministic discrete-time model for zebra mussel populations was proposed by Casagrandi. We show how this model produces periodic, stable, and chaotic population patterns. In addition, a parametric analysis corrects some results of Casagrandi concerning the effect of changes in the adult cannibalistic behavior through filter-feeding. Finally, a new stochastic continuous-time model is proposed, abstracted from the Casagrandi model and implemented via the Gillespie algorithm.

Contents

1 Introduction

As the world becomes a smaller place through the advent of better communication and transportation, the global transit of materials from one location to another has become increasingly easy. Better mobility translates to higher profits for major corporations and small businesses alike. That being said, the boom in transportation has caused impacts on the environment, as well. For instance, increased automobile emission has contributed to the air pollution problem; and the growing dependence on automobiles has furthered urban sprawl and the issues associated with that. Along a parallel line, transportation has had the effect of introducing non-native species into ecosystems around the world. It is believed that the brown rat (*Rattus norvegicus*) was introduced to New Zealand by an infestation on James Cook's ships during his circumnavigation of the island [18, pg 191]. The Colorado potato beetle (*Leptinotarsa decemlineata*) is a pest in the United Kingdom, where it is found on imported produce [3, pg 44]; and the Common Water Hyacinth (*Eichhornia crassipes*) was exported from the Amazon basin and introduced into Africa's Lake Victoria as an ornamental plant [1, pg 1]. However, perhaps one of the most prominent invasive species in the United States of America has been the zebra mussel (*Dreissena polymorpha*).

1.1 The Biology/Ecology

In order to understand zebra mussel populations and to create an accurate model, one must first understand the aspects of their biology. Ultimately, the purpose of any biological model is to mathematically recreate those aspects and grasp thier consequences. Without that knowledge, the model is just a set of equations drawn from an endless heap of many. Zebra mussels originate from the Ukrainian/Russian area of the Black Sea [16, pg 241]. The common term "zebra mussel" comes from the dark stripes present on its shell. Biologically, zebra mussels are freshwater bivavle mollusks, meaning that they have a shell split in two and joined with a ligament [15, pg 327]. Their life cycle consists of three primary stages: veliger, juvenile, and adult. Veligers are planktonic larvae that move through the use of a ciliated organelle, known as the velum [6, pg 1225]. The spawning period for zebra mussels is late spring or early summer, and a single colony of mussels is capable of producing large numbers of veligers through external fertilization [19, pg 3061]. The primary natural dispersal mechanism for zebra mussel populations is translocation in the veliger state resulting from water current flow; although adult mussels have been known to travel as a result of drifting and human vectors (e.g. recreational boating) [10, pg 248]. It is the mobility of mussel veligers that gives way to rapid dispersal of mussels in a single watershed and what makes this species so successfully invasive.

The juvenile stage begins right after the individual veliger settles and ends at sexual maturity, which occurs over a period roughly equal to two years [11, pg 429]. As a juvenile, the mussels develop byssal threads, which enables them to

attach to substrate [6, pg 1225]. Zebra mussels do not colonize all available areas of a habitat but instead attach themselves only to firm substrates (such as rocks, artificial structures, and even other mussels), although it is possible for adults to dettach and move elsewhere [19, pg 3061]. Adult female mussels are capable of producing between 30,000 and 1,610,000 eggs depending on environmental conditions [10, pg 254]. Fecundity also increases with body size [8, pg 23]. The variation in fecundity rates contributes to the extreme contrast in population levels in empirical data collected from the same location year after year [8, pg 24]. These variations are also partially due to the small survival rates from one year to the next. For the veliger population, only around 1-5% of the individual larva will survive; although some research has estimated even higher mortality rates [6, pg 1227]. Juvenile and young adults have been observed to have relatively standard survival rates; however, there is great discrepancy in life expectancies and thus the survival rates of older adult mussels. In fact, Karatayev reports the variation as 2-19 years, although how much of that is actually due to methods used in determining age or rather the biology itself is up for debate [8, pg 23]. More realistic estimates are around 4-8 years, higher in European waters and lower in North America [11, 429]

1.2 Background Information

Zebra mussels are believed to have first come to the United States by way of ballast water in the transatlantic cargo ships traveling the St. Lawrence Seaway [13, pg 2290]. They were first spotted in Lake St. Clair (Michigan/Ontario) in 1988 and were observed in all of the five of the Great Lakes by the end of 1990 [19, pg 3061]. The mussels then made their way down the Mississippi River as far as New Orleans and spread throughout much of the eastern United States, including to inland bodies of water through human-influenced vectors (as zebra mussels are capable of surving out of water for multiple days) [16, pg 239]. In fact, the spread of zebra mussels in North America was much more rapid than any one had originally thought would be the case. By 1996, the zebra mussel had invaded twenty U.S. states and two Canadian provinces, spurring the two countries' governments to fund a large body of research on the economic and ecological effects of zebra mussels, although surprisingly little was done in regards to local population dynamics [16, pgs 239-241].

Zebra mussels can have a large number of effects on an environment. Probably the biggest is biofouling. Biofouling is the unwanted accumulation of a certian population in an ecosystem (usually aquatic) which can result in increased resource competition and possible extirpation for native species. Zebra mussels are capable of extreme cases of biofouling because of their reproduction rates [13, pg 2291]. Once a zebra mussel population has been established in an area, it can be near impossible to fully remove them. Their ability to attach to almost any solid substrate increases the issue, and is ultimately the largest economic concern regarding their invasion. Zebra mussel veligers have been known to settle and develop colonies in water intake pipes of many industrial facilities, including water treatment plants, electric power stations, and steel mills [16,

pg 239-240]. Navigational buoys have sunk under the increased weight from attached mussels [19, pg 3061]. They attach themselves to docks, piers, boats, and other artifical structures. Wood, concrete, and even steel can all be structurally damaged by prolonged colonization [19, pg 3061]. Furthermore, mussels that wash up on the shore during a storm pose a potential hazard to beachgoers because of their relatively sharp shells. The 1995 National Zebra Mussel Information Clearinghouse Study reported that the 463 surveyed facilities (ranging from power plants to fisheries to golf courses) had spent $\$69,063,780.00$ on managing zebra mussel populations; and the U.S. Fish and Wildlife Service estimates that the cost will reach five billion dollars by the end of 2010 in the Great Lakes region alone [14, pg 36].

Moreover, zebra mussels can have a devastating effect on the ecosystem in which they invade. Being filter-feeders, an adult zebra mussel can filter up to a liter of water every day, pulling out particles as small as 0.7-1.0 μm [10, pgs 255-256]. This activity can remove large abundances of phytoplankton from the water, greatly affecting the food web [19, pg 3061]. In addition to the phytoplankton, zebra mussels filter out contaminants found in the water and build up those toxins in their system. Waterfowl and other predators who consume zebra mussels also consume these toxins, resulting in sometimes devistating effects including reduced reproduction [16, pg 240].

All of that being said, zebra mussels have done a number of things that could be considered as positive for the ecosystems in which they invade. As previously stated, their filtering activity results in clearer water with less toxins and other harmful material. In fact, there is a current project underway in Michigan that uses zebra mussels to monitor E. coli in the Clinton River [4, pg 2]. The mussels filter out the bacteria at a continuous rate and can reveal E. coli concentrations better than just testing the water directly. Clearer water also gives way to increased sunlight penetration, which contributes to greater numbers of benthic animals and macrophytes [16, pg 240]. As a result, the population of adult yellow perch (which are benthivorous fish) in Lake St. Clair has shown a positive growth rate since the introduction of zebra mussels; while without the mussels, yellow perch were loosing biomass [5, pg 1914].

2 Methods

A large amount of the energy put towards researching zebra mussels has dealt with the effects of zebra mussel populations, rather than trying to understand the populations themselves. There is an abundance of papers dedicated to the costs associated with zebra mussels and the competition between the mussels and native species. Thus, in an attempt to better comprehend the local population dynamics, this paper explores several different models. The first is a density-dependent deterministic discrete-time model. To better understand the subtleties of the model, a parametric study is performed and the possibility of calculating an intrinsic growth rate for zebra mussel populations is discussed. The second is a new stochastic model abstracted from the Gillespie algorithm

over a randomized time field and is intended to expand upon the first. All computational work for both models was implimented in the C programming language [17] and Stata Data Analysis and Statistical Software [9].

2.1 Deterministic Model

The model presented first in this paper is a density-dependent deterministic discrete-time model that was first introduced by Casagrandi in 2007, though it is partially based on the 1954 Ricker model that exhibited the self-cannibalistic tendencies of fish populations.

2.1.1 Equations

The model takes the following mathematical form [6, pg 1226]: gillespie algorithm time exponential

$$n_1(t+1) = \sigma_0 exp\big[-\beta N(t)\big]\left[\frac{f_2 n_2(t)}{2} + \frac{f_3 n_3(t)}{2} + \frac{f_4 n_4(t)}{2}\right] \tag{1a}$$

$$n_2(t+1) = \sigma_1 n_1(t) \tag{1b}$$

$$n_3(t+1) = \sigma_2 n_2(t) \tag{1c}$$

$$n_4(t+1) = \sigma_3 n_3(t) + \sigma_4 n_4(t) \tag{1d}$$

The zebra mussel population is divided into four separate stages: $n_i(t)$ represents the number of zebra mussels of Stage i at time t, whereas $N(t) = n_1(t) + n_2(t) + n_3(t) + n_4(t)$ is the total zebra mussel population at time t. As a consequence of the varied life expectancies of zebra mussels as explained in Section 1.1, those mussels staged 4 and larger have been catagorized into the same class ($n_4(t)$). Hence, Equation (1d) promotes mussels from Stage 3 but also retains those already in Stage 4+. In the literature, more often than not the word "Age" will be used instead of the term "Stage" which would seem to make sense with the yearly promotion of each grouping. However, in the field, zebra mussels are catagorized based on observed physical characteristics; thus, the "Stage" is considered to be more appropriate terminology. Biologically, referring to Stage 1 would be the same as referring to the juvenile population. Stages 2, 3, and 4+ reflect successively older and larger zebra mussel groupings. This results in a more biologically accurate model, as breaking up the adult population allows different parameter values to be assigned to mussels that would realistically be performing at different rates.

The σ_i parameters are the survival rates as one stage is promoted to the next every year. So, σ_1 in Equation (1b) is the rate at which Stage 1 mussels survive to Stage 2, and so on and so forth. That being said, σ_0 in Equation (1a) has a slightly deeper meaning: $\sigma_0 = \sigma_E \times \sigma_V$, where σ_E is the rate at which eggs are fertilized by adult males and σ_V is the survival rate of veligers in a low density of adult mussels. The exponential term found in the same equation is what has been adapted from the Ricker model, meaning that this accounts for the canabalistic tendencies found in the system as a result of filter-feeding.

The parameter β represents the filtration rate by adult zebra mussels. The final term in that equation can be thought of as an average population of veligers. f_i is the fecundity, or the average number of eggs released by one adult female of Stage i. Thus, $f_i n_i(t)/2$ is the total number of vilegers produced by the Stage i mussels, assuming that the gender ratio is roughly equal. Only female zebra mussels of Stage 2 or greater can produce eggs so Stage 1 has been excluded from this term.

Parameter	Value	Description
σ_0	0.01	combined rate of veliger survival and birth
σ_1	0.88	survival rate of Stage 1 mussels to Stage 2
σ_2	0.41	survival rate of Stage 2 mussels to Stage 3
σ_3	0.35	survival rate of Stage 3 mussels to Stage 4+
σ_4	0.04	retention rate of Stage 4+ mussels
f_2	0.24×10^6	fecundity of Stage 2 female mussels
f_3	0.465×10^6	fecundity of Stage 3 female mussels
f_4	0.795×10^6	fecundity of Stage 4 female mussels
β	1.0	filtration rate of adult mussels

Table 1: The Parameter Set. Alterations made to these parameter values are explicitely mentioned where they occur.

Using this model and the parameters found in 1 which were originally set by Antonni [2], we have been able to reproduce the results of Casagrandi. However, there was some difficulty in producing these graphs. In Casagrandi's article, the parameters used are explicitly outlined; however, the initial conditions are rather ambiguous. From visual inspection, the graphs appear to have an initial population of around $N(0) = 120$ zebra mussels; however, after some analysis was done using various populations and combinations of different ages, we were unable to produce graphs that exactly matched Casagrandi's. Thus, these graphs were created using the same parameter values but different initial populations to reflect similar patterns to those found in the 2007 article. Initial conditions have been set such that $n_1(0) = n_2(0) = n_3(0) = n_4(0) = 20$. Thus, $N(0) = 80$ is the total abundance of zebra mussels at the start of the model. This initial condition is realistic for when a population is considered some time after already being introduced into an area. As previously mentioned, it is common for only a select amount of the veliger population to be first introduced because of their mobility. Thus, an analysis exploring the outbreak of an invasive population might have a large number of Stage 1 mussels with little or no Stage 2, 3, or 4+. However, the goal of this analysis is to understand the population dynamics over a set period of time, rather than the initial invasion of mussels. Thus, these initial population values are used.

It is important for a universal zebra mussel population model to be versatile in its ability to create different behavioral patterns. Unlike many other living things, zebra mussels can have vastly different population behaviors based on the location of the colony, which has caused difficulty in modeling their local dy-

namics. This variance originates mostly from environmental conditions, such as salinity, pH, temperature fluctuations, and levels of different chemicals present in the water [12, pg 357-358]. The three most prominant behavioral patterns are chaotic, cyclic (of varied periods), and stable. One of this model's key strengths is its ability to produce all three of these patterns.

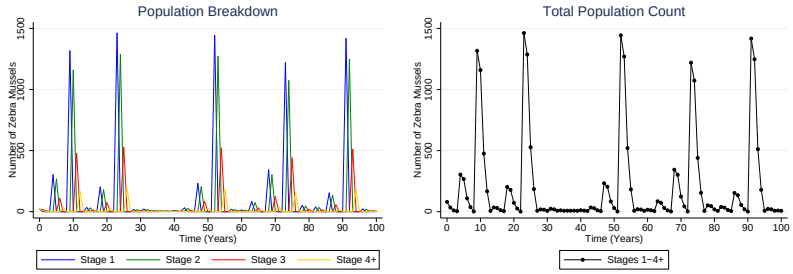

Figure 1: Population Breakdown and Total Population - Chaotic. Parameter set found in Table 1. Random peak height and timing.

Figure 1 corresponds to the seemingly random sequences found in empricial data collected on zebra mussels, a pattern sometimes referred to as "chaotic regime". The population spikes irregularly and without warning, or in other words the peaks of the graph can vary in height considerably and are not at regular time intervals. The graph also exhibits the ability for the population to lie "dormant" for some time (specifically speaking about $27 \leq t \leq 46$, where the population never goes above 35 mussels for almost 20 years).

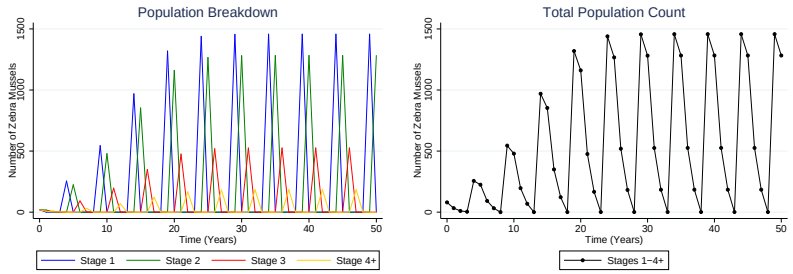

Figure 2: Population Breakdown and Total Population - Cyclic One. $\sigma_4 = 0.005$. 5-year cyclic pattern, increase to a constant peak height.

Figures 2 and 3 reflect cyclic populations. Zebra mussels have been observationally shown to be periodic in different regions of the world; and as might be expected, the periods of these observations are often different. Depending on the parameter set, this model will exhibit not only cyclic behavior, but also cycles of different length. Figure 2 has a period of five years. Also note the increase to

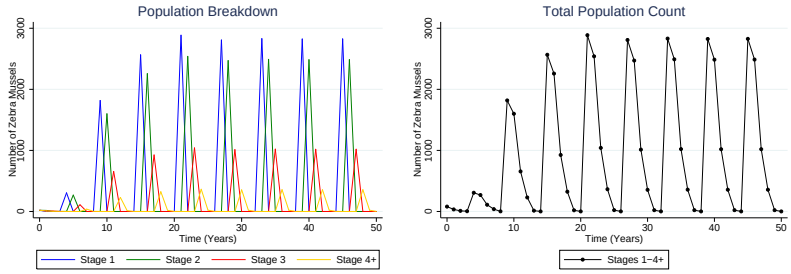

Figure 3: Population Breakdown and Total Population - Cyclic Two. $\sigma_0 = 0.02$ and $\sigma_4 = 0.06$. 6-year cyclic pattern, increase to a constant peak height.

a constant peak height of just below 1,500 mussels over time. In contrast, Figure 3 has periods of six years, and levels out to a population almost twice that found in Figure 2. Figure 4 is also noteworthy. In it, the population reaches an equilibrium value of around 88 mussels in a relatively short period of time after a bit of fluctuation. Zebra mussel populations have been observed at relatively constant levels for extended periods of time. Thus, a complete model must also be able to exhibit a stable population pattern, as the Casagrandi model does - once again dependent on the parameter set.

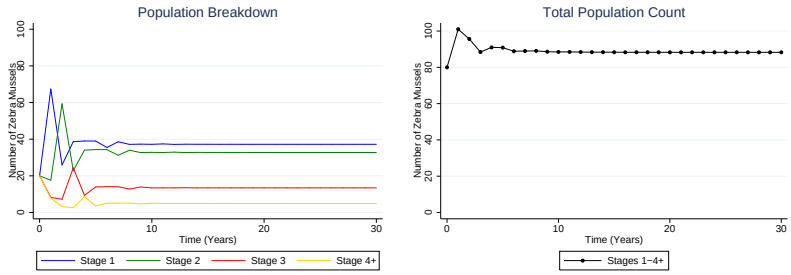

Figure 4: Population Breakdown and Total Population - Equilibrium. $\sigma_0 = 0.00001$ and $\beta = 0.01$. Stable pattern, levels out to a constant population.

A final point of discussion is just how the populations evolve in this model. A feature in all of the graphs (with the exception of the equilibrium found in Figure 4) is that when a spike in population occurs, the resulting next few years experience a decline in population as a direct consequence of the survival rates from Stage (i) to Stage $(i+1)$. Also, there is never a sizable influx to the population immediately after a peak because the exponential term in (1a) is close to 0 as a result of a large $N(t_p)$, where t_p is the time at which the population peaks. Biologically speaking, the high number in total population means for a large amount of filter-feeding. In turn, this results in a large amount of canabalism on the veliger population and thus no increase in population even

though the mature females will produce a vastly large number of eggs in total.

Even more interesting is why the populations spike in the first place. It is also a direct outcome of the filtering. The total population must reach a low enough level where the filtering has little to no effect on the veliger population's survival. Only then can the veligers have the hope of making it to Stage 1. Then, as a result of high reproduction rates, the population will spike to numbers sometimes 1,000 times or more than it was previously. All of this means that the total population of zebra mussels in this model tends to move in a sequence reminiscent of a wave. A grouping of mussels will move through time as the dominant Stage from year to year until eventually enough die that a new group can emerge, only to repeat the same pattern. When the parameter set dictates periodic behavior, this occurs on a regular cycle. On the other hand, when the parameters result in a chaotic pattern, this sequence is more randomized. The only exception to this rule being when parameters allow for an equilibrium.

2.1.2 Parameter Anaylsis

Much of Section 2.1.1 was devoted to explaining the Casagrandi model and reviewing the aspects of the model that make it liable to local zebra mussel population dynamics. So, although parameter values were specified and described, very little emphasis was given to understanding parameteric sensitivity. Thus, further analysis will be given specifically to the σ_i and β values with an emphasis on the different temporal structures.

Turing attention first towards the σ_i values, Casagrandi argues that only σ_0 and σ_4 are of importance to the model [6, pg 1227]. Survival of Stage 1 mussels to Stage 2 (σ_1), Stage 2 mussels to Stage 3 (σ_2), and Stage 3 mussels to Stage 4+ (σ_3) mostly control the rate of post-peak population decline, which is ultimately of little consequence when considering the overall pattern. The population spikes are most sensitive to veliger survival and the retention of Stage 4+ mussels.

Veliger survival controls whether or not the population is even able to spike because mussels are only introduced through reproduction (as opposed to including adult translocation). As a result of the empirically low veliger survival, values for σ_0 were constrained to $0 - 5\%$. Retention of Stage 4+ mussels is important for two reasons. The first of which is that they are the mussels with the highest fecundity rates and thus capable of producing the most veligers. Secondly, retention of Stage 4+ mussels varies so much from location to location. Areas with high retention rates experience increased canabalistic effects, and the reverse is true for areas with low retention rates. The biological variance makes σ_4 difficult to realistically bound. σ_4 will be small in areas with shorter lifespans and large in locations where mussels are known to live longer. For sake of argument, σ_0 is examined for $0 - 10\%$. This value is more relatable to North American populations of zebra mussels, as they are known to have shorter life expectancies than the European colonies.

Figure 5 is the result of analysis of the graphs generated using different σ_0, σ_4, and β values and can be thought of as a diluted bifurcation diagram.

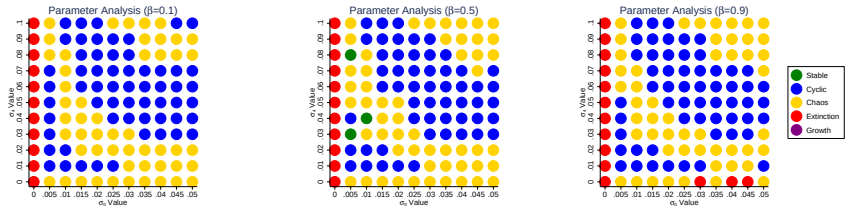

Figure 5: Multidimensional Parameter Analysis. Left to right: $\beta = 0.1$; $\beta = 0.5$; and $\beta = 0.9$.

Parameter sets were made for every possible combination $0.0 \leq \sigma_0 \leq 0.05$ with a step size of 0.005, $0.0 \leq \sigma_4 \leq 0.1$ with a step size of 0.01, and $0.0 \leq \beta \leq 1.0$ with a step size of 0.1. The behavioral pattern was manually examined and recorded for each parameter set; and a color scale is used to differentiate five different population scenarios (Stable, Cyclic, Chaos, Extinction, or Growth). This analysis produced a result simlar to that found in Casagrandi's parameter analysis [6, pg 1228]. In all three graphs, there are obvious banded regions. These markings indicate blocks where diferent temporal structures occur. A more complete bifurcation analysis would reveal the exact curves where the behavior changes. The red line on the left is where $\sigma_0 = 0.0$, meaning that none of the veliger population survives, so extinction is the expected result.

Although it is not pictured, unbounded growth occurs where $\beta = 0.0$ and $\sigma_0 \neq 0.0$. If $\beta = 0.0$, then the exponential term that accounts for filtration and the canabalism of veligers is effectively removed from the system. This is also a major term restricting population growth. So, the case where $\beta = 0.0$, will be omitted from further analysis. Similarly, parameter sets involving stable populations will also be omitted as a stable population will not illustrate population peaks by definition.

Removing the case where $\beta = 0.0$, Casagrandi contends that changing β has little effect on the model, except for the height of the population peaks [6, pg 1226-1227]. Indeed, even a cursory analysis leads one to believe β has a direct relation to the peak height. Figure 5 would seem to suggest something similar, as there is little variation between the graphs with different β values. However, further investigation argues a more subtle result. By altering β and holding all else constant, there was a great effect on the placement and number of peaks over a given timespan, which is of obvious importance in determining population size at any given time and certianly important in terms of the overall patterns present.

Analysis was made using three different parameter sets, identical to those used in generating the graphs found in Section 2.1.1. As shown in Figures 1, 2, and 3, two of the parameter sets produce cyclic patterns and the third produces a chaotic pattern. Data sets mapping the total population were generated for fifty years using each of the parameter sets with increments of 0.01 on $0.0 < \beta \leq 1.0$. The times for the highest peaks were recorded for each data set and then plotted

against their corresponding β value.

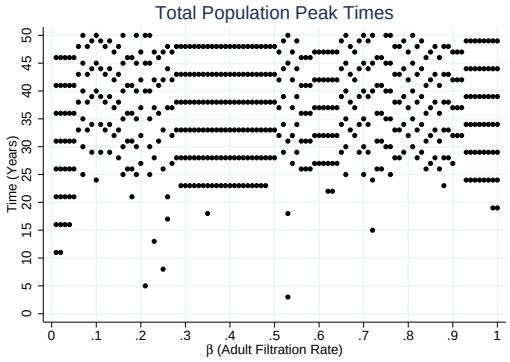

Figure 6: Total Population Peak Times - Cyclic One. $\sigma_4 = 0.005$.

Figure 6 is the resulting graph for one of the cyclic parameter sets. Indeed the periodic nature is evident in the graph; for a single β value, the time between each successive peak is on average the same. Probably the most salient feature of this graph is the horizontal lines present. They argue that the top population peaks occur at regular time intervals and for the most part occur at the same year marks (t = 23, 28, 33, 38, 43, and 48). These results correspond with Casagrandi's statement, as these are where alteration of β has no effect on the overall peak structure in terms of timing.

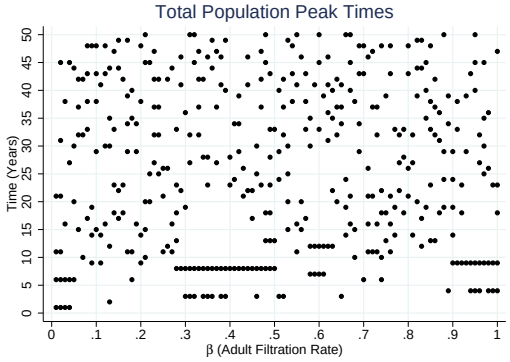

Figure 7: Total Population Peak Times - Chaos. Parameter set found in Table 1.

In contrast to Figure 6, Figure 7 was generated using a parameter set for chaotic behavior. Surprisingly enough, horizontal lines can still be found on the graph, although distinctly less of them. The randomized "cloud" of dots in the upper half of the figure corresponds to areas where changes in β influences

the population peak timing. One might be led to argue that the prominent horizontal lines (and thus identical peak structure) are a consequence of cyclic parameters which would seem to make sense. However, Figure 8 also uses cyclic parameters. Its pattern, although still cyclic, pushes away from that found in Figure 6 and closer to the chaotic pattern. It has less horizontal line patterns and more areas of randomization. Thus, similar temporal structure is not necessarily a direct result of cyclic parameters (although the two are at least related). As a final realization, it can be definitively concluded that β alters peak structure more than just in terms of height.

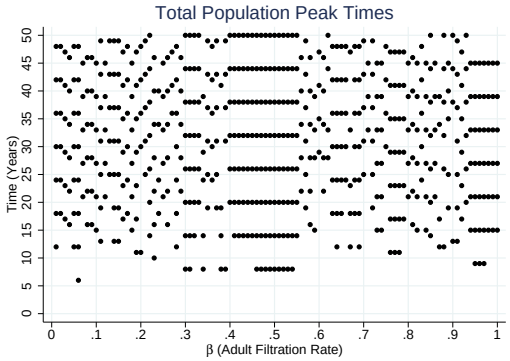

Figure 8: Total Population Peak Times - Cyclic Two. $\sigma_0 = 0.02$ and $\sigma_4 = 0.06$.

Combining the results of the β analysis and the σ_i analysis, Casagrandi's parametric study is found to be correct with regards to behavioral patterns; however, it falls short in regards to the specifics. While the pattern is important, a practical universal model to track zebra mussel populations with so many different parameters must be accompanied by an analysis of how not just the pattern changes with alterations of the parameter values but also an analysis of how temporal structure and peak height change.

2.1.3 The Intrinsic Growth Rate

The intrinsic growth rate of a population is the measure at which the population grows on average over an extended period of time. Note that for an equilibrium parameter set, the growth rate is irrelevant, since the population by definition is constant. Similarly, by definition a chaotic parameter set is too random to have a general growth trend. Thus, when talking about the intrinsic growth rate, reference is made to the parameter sets where the population pattern is periodic.

The first step in attempting to determine the model's intrinsic growth rate is to establish upper and lower bounding functions on the graph. In this case, the process is a little more subtly complicated than one might expect. Starting with the original set of equations found in Section 2.1.1, sum them together to

have an equation for $N(t+1)$:

$$\begin{aligned} N(t+1) &= \sigma_0 exp\big[-\beta N(t)\big]\left[\frac{f_2 n_2(t)}{2} + \frac{f_3 n_3(t)}{2} + \frac{f_4 n_4(t)}{2}\right] + \\ &\quad \sigma_1 n_1(t) + \sigma_2 n_2(t) + \sigma_3 n_3(t) + \sigma_4 n_4(t) \end{aligned}$$

The bottom line of the right hand side of the equation (which comes from the sum of Equations (1b), (1c), and (1d)) is the easier section to bound. First, note that if all of the σ_i values were the same, then this whole term would just be equal to $\sigma_i N(t)$. Thus, we can bound the upper limit of this section by taking the maximum σ_i value and multiplying it by $N(t)$. Similarly, the lower bound can be found using the minimum σ_i value. Thus, written mathematically:

$$\sigma_{min} N(t) \leq \sigma_1 n_1(t) + \sigma_2 n_2(t) + \sigma_3 n_3(t) + \sigma_4 n_4(t) \leq \sigma_{max} N(t).$$

Now, consider the first half of the equation (which is really just Equation (1a)). First, factor out the $\frac{1}{2}$ from the bracketed section with fecundities:

$$\frac{\sigma_0}{2} exp\big[-\beta N(t)\big]\big[f_2 n_2(t) + f_3 n_3(t) + f_4 n_4(t)\big].$$

Then, replace the $n_i(t)$ terms using Equations (1b), (1c), and (1d) evaluated at time t (and thus expressed in terms of $(t-1)$):

$$\frac{\sigma_0}{2} exp\big[-\beta N(t)\big]\big[f_2\sigma_1 n_1(t-1) + f_3\sigma_2 n_2(t-1) + f_4\big(\sigma_3 n_3(t-1) + \sigma_4 n_4(t-1)\big)\big].$$

Similarly to before, notice that if all of the $f_i\sigma_j$ terms were the same, the equation could be expressed in terms of $N(t)$ in the exponential term and $N(t-1)$ in the latter section. Thus, by taking the maximum and minimum values in the set $\{f_2\sigma_1,\ f_3\sigma_2,\ f_4\sigma_3,\ f_4\sigma_4\}$, upper and lower bounds for this section are outlined. Once again, expressed mathematically:

$$\begin{aligned} &\frac{\sigma_0}{2} exp\big[-\beta N(t)\big](f\sigma)_{min} N(t-1) \leq \sigma_0 exp\big[-\beta N(t)\big] \times \\ &\quad \left[\frac{f_2 n_2(t)}{2} + \frac{f_3 n_3(t)}{2} + \frac{f_4 n_4(t)}{2}\right] \leq \frac{\sigma_0}{2} exp\big[-\beta N(t)\big](f\sigma)_{max} N(t-1). \end{aligned}$$

Now, combining the results of bounding both of the sections, the bounds for the entire $N(t+1)$ equation are written:

$$\begin{aligned} \sigma_{min} N(t) + \frac{\sigma_0}{2} exp\big[-\beta N(t)\big](f\sigma)_{min} N(t-1) &\leq N(t+1) \\ &\leq \sigma_{max} N(t) + \frac{\sigma_0}{2} exp\big[-\beta N(t)\big](f\sigma)_{max} N(t-1). \end{aligned}$$

The most noteworthy thing about these bounding functions is their use of two initial conditions; one needs to know both $N(t-1)$ and $N(t)$ in order to bound $N(t+1)$. In this way, the bounding equations are said to have two levels of memory. In practice, this can generate an extra problem to deal with;

finding one initial condition is difficult enough, let alone two. The process used in this paper is rather simple. The algorithm employed makes use of the single set of initial conditions given to the model and then uses the model equations (1) to generate a second set at $t = 1$. Thus, for both $t = 0$ and $t = 1$, the upper and lower bounds are equal to the function being bounded; however, for t values greater than that, the bounds fall above and below the predicted values, respectively.

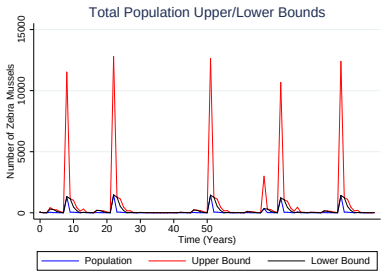

Figure 9: Population Upper/Lower Bounds - Chaos. Parameter set found in Table 1.

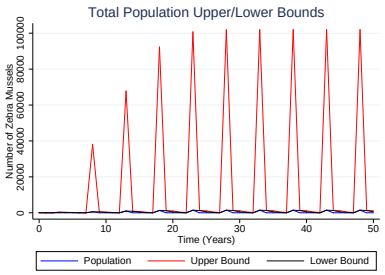

Figure 10: Total Population Upper/Lower Bounds - Cyclic One. $\sigma_4 = 0.005$.

After establishing the bounding functions, the first question to ask is how well they compare to the predicted values from the model. Looking at the Equilibrium graph in Figure 12, one might argue that they don't bound the population curve well at all; the bounds are well above and below the population value. However, looking at the other three graphs in Figures 9, 10, and 11, the bounding functions seem to almost dictate the population level which ultimately reveals the complex sensitivity of the model.

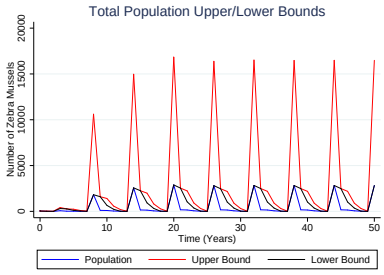

Figure 11: Total Population Upper/Lower Bounds - Cyclic Two. $\sigma_0 = 0.005$.

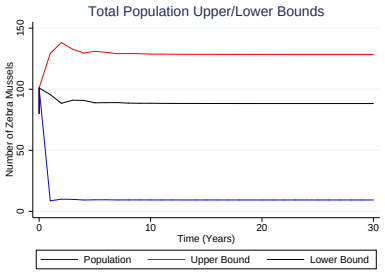

Figure 12: Total Population Upper/Lower Bounds - Equilibrium. $\sigma_0 = 0.00001$ and $\beta = 0.01$.

In each graph all three curves exhibit population spikes at the same time, which makes sense as to how the bounding functions were derived. What is

remarkable is that where the population spikes, the lower bound seems to control how high the population will initially spike; whereas the upper bound seems to control how the population declines after the spike. In fact, if once again t_p is the time at which the population peak occurs, the lower bound at t_p is the same value as the model population for all practical purposes. Furthermore, at time $(t_p + 1)$, the population matches the value of the upper bound. This is most obvious in the Cyclic Two graph in Figure 11.

Unfortunately, the ultimate conclustion after finding the bounding functions is that there is no intrinsic growth rate for zebra mussel populations (at least in this model) because of the "boom and bust" dynamics present. Even with the bounding functions, the patterns are simply too periodic; and with this periodicity, an intrinsic growth rate is simply impossible to calculate.

2.2 Stochastic Model

When examining the literature, there were many papers detailing the effects of zebra mussels; however, very few trying to understand the sometimes cyclic, sometimes chaotic, and sometimes stable patterns so present in the empirical data. Casagrandi did such with a discrete deterministic model; however his article did not directly outline a stochastic model to produce similar results. Thus, the next model presented in this paper attempts to fill that void. It is a stochastic model over a randomized time field and is fashioned loosely from the deterministic model in Section 2.1.1, although it uses an algorithm adapted from Gillespie [7].

2.2.1 The Algorithm

The algorithm is designed to correlate with the zebra mussel life cycle. Using the same groupings as the deterministic model, it starts with an initial population and outlines a series of possible events that could happen to that population and accounts for each of these events. Those possibilities are as follows: (1) maturation of a veliger; (2) death of a veliger; (3) promotion of an Stage 1 mussel to Stage 2; (4) death of an Stage 1 mussel; (5) promotion of an Stage 2 mussel to Stage 3; (6) death of an Stage 2 mussel; (7) promotion of an Stage 3 mussel to Stage 4+; (8) death of an Stage 3 mussel; (9) survival of an Stage 4+ mussel; (10) death of an Stage 4+ mussel. Each one of these events happens with a different probability (as it is reasonable to assume that some events are more likely to happen than others). The model assumes that events won't happen simultaneously. For simplification purposes, events (1) and (2) will be absorbed into what will account for the annual spawning of the population; and we will only allow events (3) - (10) to occur throughout the year.

According to Gillespie, there are two things to generate when looking at a stochastic model. The first is when the next event will occur, and the second is what that event will be. Determining the time is done through generation of a pseudorandom number between 0 and 1 using an exponential distribution, scaled to the probability of the events. The result is considered Δt and added

to the previous t value, starting with $t = 0$. This is then iterated for the next event possibility over and over again until a maximum value of t is attained.

Secondly, the algorithm must randomly determine which event happens. This is done using the probability of each event in relation to the other events. These probabilities come from the σ_i values in the Casagrandi model. The probability a Stage i zebra mussel will be promoted/survive is equal to σ_i, whereas the probability that it will die is equal to $(1 - \sigma_i)$. These numbers are then scaled down such that their values add up to 1 and then laid out next to each other on a theoretical number line. Once again, a pseudorandom number between 0 and 1 is generated and compared to the number line. The number generated will fall in the range of probability for a given event, and that event is what is determined to happen. Finally, the population change is marked and the process is iterated for each generated t value.

So now the question becomes how the spawning period should be dealt with. The model was coded such that it would determine whenever the time passed an integer value of time, which is defined to be the time of year spawning occurs. When this is the case, the model adds

$$\sigma_0 exp\big[-\beta N(t)\big]\big[\frac{f_2 n_2(t)}{2} + \frac{f_3 n_3(t)}{2} + \frac{f_4 n_4(t)}{2}\big]$$

to the n_1 class. This results in correctly modeling the spawning period once every year. It is worthwhile to note that events (1) and (2) have been factored into this process as they were in the deterministic model, rather than being dealt with explicitly as events (3)-(10) have been.

2.2.2 The Trials

Monte Carlo Trials were run in an attempt to gather further information. As with the deterministic model, initial conditions were set at $n_1(0) = n_2(0) = n_3(0) = n_4(0) = 20$. The same parameter sets as in the deterministic model were also used in the stochastic case. This allows for comparisons to be made between the two models, as well as the examination of the three different behavioral patterns: chaotic, cycilc (of varied periods), and stable. Although many more trials were run, a set of ten random trials were chosen and then plotted for each parameter set. In addition, the population number of these ten trials were averaged together at every integer value of time; and then that line was also plotted in the graph to offer an overall view of the population dynamics. When examining the graphs produced using these methods, it is important to remember the random and varying nature of a stochastic process.

Looking at the graph with a chaotic parameter set (found in Figure 13), one will note that there is a great deal of variance in the individual trials. This would make sense, as the nature of chaos is to have randomized and unpredictable population spikes to varying heights. In fact, this result is parallel to that found in the deterministic model. The average line follows the trends found in all of the other lines, spiking whenever there is a spike no matter which individual curve is spiking.

When looking at graphs generated with cyclic parameters, there are two specific points of interest. The first is similar peak height, and the second is groupings of peaks in the individual trials. The Cyclic One case found in Figure 14 better exemplifies this than the Cyclic Two case found in Figure 15. In the Cyclic One graph, there is noticable bunching of peaks in every case where the average line spikes. This would argue that the each of the Monte Carlo Trials is producing similar temporal patterns. In addition, the population peaks rise to roughly the same value every time (with of course some error by the very nature of a series of stochastic processes). In the Cyclic Two graph, these characteristics are slightly less evident, although still present.

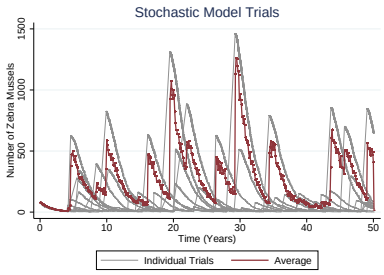

Figure 13: Monte Carlo Trials - Chaos. Parameter set found in Table 1.

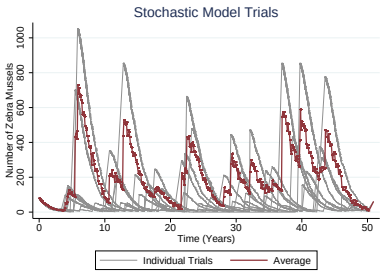

Figure 14: Monte Carlo Trials - Cyclic One. $\sigma_4 = 0.005$.

Finally, the Equilibrium graph in Figure 16 is of great interest. Note that the individual trials seem to fluctuate a substantial amount. Although when the average curve is examined, it can be seen that this fluctuation decreases considerably. In fact, in this set of trials, the average curve seems to account for a population around 90 zebra mussels with fluctuations of around 20 mussels, which closely matches the value in the deterministic model.

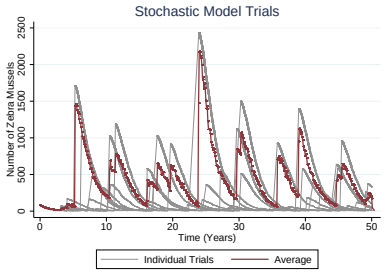

Figure 15: Monte Carlo Trials - Cyclic Two. $\sigma_0 = 0.02$ and $\sigma_4 = 0.06$.

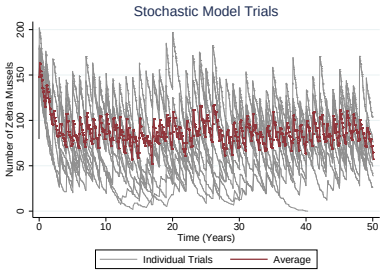

Figure 16: Monte Carlo Trials - Equilibrium. $\sigma_0 = 0.00001$ and $\beta = 0.01$.

Similar results to these were found when more and more Monte Carlo Trials were performed with each parameter set. That being said, there was of course some dissimilarity in all of the trials, as would be expected. In some of the generated trials, populations were led to extinction which is a valid biological outcome. However, this is something that cannot be acheived with the deterministic model using the given parameter sets. The other large observed variation had to do with the cyclic trials. While they all seemed to follow some sort of loose pattern, in many of the trials this sequence was less defined than might have been hoped for. Looking at the stochastic cylic graphs in comparison to those of the deterministic model, it is unmistakable that the temporal patterns are less regularly cyclic. However, it would be easy to argue that the stochastic model simply reflects a more natural sequence.

3 Conclusion

Casagrandi's model successfully generates chaotic, cyclic (of varied periods), and stable local population dynamics for zebra mussel colonies. Depending on the parameter set, it is able to produce realistic population levels and account for the cannabalistic nature of the filter-feeding process. The parametric study found in this paper validates the work of Casagrandi regarding the σ_i values and corrects the work done concerning β. Moreover, although an intrinsic growth rate cannot be found because of the periodicity, the model is definitely creditable when the boom and bust dynamics of the empirical data is considered.

The stochastic model abstracted from Casagrandi and the Gillespie algorithm explores zebra mussel populations in what may be considered a more natural sense than the deterministic model. Its use of a randomized field for time and a random selection process for events better simulates reality. The relative success of iterated trials reinforces this notion. Additionally, it helps to fill a void in the literature with regards to modeling local dynamics.

Further work could be done on this topic and specifically with the work presented in this paper. It is possible to abstract the model to include a spatial component in order to predict the location of individual zebra mussels and mussel buildup within an ecosystem; however, local environmental dimensions would need to be known. It is also possible to expand this study to include patch-to-patch dynamics in order to model the spread of zebra mussel populations over a single watershed, or even over larger areas of land - for instance the North American continent. However, the lack of these components does little to affect the validity of this model, as local population dynamics must be formally understood before such attempts can even be made.

References

[1] The curse of the water hyacinth. *Economist*, 346(8050):68 – 69, 1998.

[2] D. Annoni, I. Bianchi, A. Girod, and M. Mariani. Inserimento di dreissena polymorpha (pallas)(mollusca bivalvia) nelle malacocenosi costiere del lago di garda (nord italia). *Quaderni della Civica Stazione Idrobiologica di Milano*, 6:5–84, 1978.

[3] P. W. Bartlett. Colorado beetles reported in england, wales and scotland, 1975. *Plant Pathology*, 25(1):44 – 47, 1976.

[4] Helen Buttery. In praise of a pest. *Maclean's*, 114(41):61, 2001.

[5] Renato Casagrandi, Lorenzo Mari, and Marino Gatto. Zebra mussel (dreissena polymorpha) effects on sediment, other zoobenthos, and the diet and growth of adult yellow perch (perca flavescens) in pond enclosures. *Canadian Journal of Fisheries and Aquatic Sciences*, 54(8):1903–1915, August 1997.

[6] Renato Casagrandi, Lorenzo Mari, and Marino Gatto. Modelling the local dynamics of the zebra mussel (dreissena polymorpha). *Freshwater Biology*, 52(7):1223–1238, July 2007.

[7] Daniel T. Gillespie. Exact stochastic simulation of coupled chemical reactions. *The Journal of Physical Chemistry*, 81:2340–2361, May 1977.

[8] Alexander Y. Karatayev, Lyubov E. Burlakova, and Dianna K. Padilla. Growth rate and longevity of dreissena polymorpha (pallas): A review and recommendations for future study. *Journal of Shellfish Research*, 25:23–32, April 2006.

[9] StataCorp LP. Stata statistical software: Release 11, 2009.

[10] Gerald L. Mackie and Don W. Schloesser. Comparative biology of zebra mussels in europe and north america: An overview. *American Zoologist*, 36(3):244–258, 1996.

[11] Lorenzo Mari, Renato Casagrandi, Maria Teresa Pisani, Emiliano Pucci, and Marino Gatto. When will the zebra mussel reach florence? a model for the spread of ¡i¿dreissena polymorpha¡/i¿ in the arno water system (italy). 2(4), 2009.

[12] Robert F. McMahon. The physiological ecology of the zebra mussel, dreissena polymorpha, in north america and europe. *American Zoologist*, 36(3):339–363, June 1996.

[13] Kristen M. Nelson, Carl R. Ruetz, and Donald G. Uzarski. Colonisation by dreissena of great lakes coastal ecosystems: how suitable are wetlands?. *Freshwater Biology*, 54(11):2290 – 2299, 2009.

[14] Charles R. O'Neill Jr. Economic impact of zebra mussels - results from the 1995 national zebra mussel information clearinghouse study. *Great Lakes Research Review*, 3(1), April 1997.

[15] Jeffrey L. Ram, Peter P. Fong, and David W. Garton. Physiological aspects of zebra mussel reproduction: Maturation, spawning, and fertilization. *American Zoologist*, 36(3):326–338, June 1996.

[16] Jeffrey L. Ram and Robert F. McMahon. Introduction: The biology, ecology, and physiology of zebra mussels. *American Zoologist*, 36(3):239–243, June 1996.

[17] Herbert Schildt. *Teach Yourself C*. Osborne McGraw-Hill, Berkeley, CA, 1990.

[18] Rowland H. Taylor and Bruce W. Thomas. Rats eradicated from rugged breaksea island (170 ha), fiordland, new zealand. *Biological Conservation*, 65(3):191 – 198, 1993.

[19] Levente Timar and Daniel J. Phaneuf. Modeling the human-induced spread of an aquatic invasive: The case of the zebra mussel. *Ecological Economics*, 68(12):3060 – 3071, 2009.